

J. BARAN,¹ M. DROZD,¹ T.A. GAVRILKO,² V.I. STYOPKIN²¹Institute of Low Temperatures and Structure Research, PAN
(2, Okolna Str., Wroclaw, Poland)²Institute of Physics, Nat. Acad. of Sci. of Ukraine
(46, Prosp. Nauky, Kyiv 03068, Ukraine; e-mail: gavrilko@iop.kiev.ua)**STRUCTURE, MOLECULAR DYNAMICS,
AND THERMOTROPIC PROPERTIES OF STEARIC
ACID-CTAB CATIONIC SURFACTANTS
WITH DIFFERENT MOLAR RATIOS**PACS 61.05.Cp, 61.66.Hq,
64.70.Kt, 65.40-b

Solid phase complexes containing cetyltrimethylammonium bromide (CTAB) $[H_3C-(CH_2)_{15}-N^+(CH_3)_3]Br^-$ (cationic surfactant) and stearic fatty acid (SA) $(H_3C-(CH_2)_{16}-COOH)$ (anionic surfactant) were prepared with different SA:CTAB molar ratios ranging from 4:1 to 1:4. The prepared catanionic (CA) surfactants are characterized by using X-ray powder diffraction, DSC analysis, and temperature-variable FTIR spectroscopy. It is shown that the obtained CA complexes in the solid state are assembled into a phase-segregated layered structure. The aggregate composition is close to equimolar with the coexisting excessive SA or CTAB phase, which is confirmed by FTIR spectroscopy. Complicated phase behaviors depending on the SA:CTAB molar ratio are observed in these systems. Upon heating, a series of phase transitions occurs, yielding finally an orientationally disordered hexagonal structure. With DSC analysis, the greatly enhanced stability of the complexes (particularly, the 1:1 one) over pure acid (by about 40 °C) is found. The structural effects on the phase diagram and the molecular dynamics of SA:CTAB aggregates are discussed.

Keywords: X-ray diffraction, DSC, FTIR spectroscopy, CTAB, stearic acid; solid phase catanionics.

1. Introduction

Recently, the binary mixtures of oppositely charged cationic and anionic surfactants, the so-called catanionic surfactants (CAS), have attracted a lot of interest due to their remarkable ability to form a variety of self-assembled structures both in water and in air-water or air-solid interfaces, and are of great application potential in nanotechnology for the synthesis of various nanoobjects, as well as for various encapsulation and controlled-delivery processes in pharmacy, medicine, and biology [1–3]. Structure, morphology, and properties of CAS depend on many factors, including properties of the initial surfactants, their molar ratio, type of a solvent, etc. Systems of CAS containing fatty acids (R-COOH) with different cationic surfactants (cetyltrimethylammonium bromide (CTAB) $[H_3C-(CH_2)_{15}-N^+(CH_3)_3]Br^-$, amines (R-NH₂) have been intensively studied [4–8]. In [8], it was shown that CAS consisting of unde-

canoic acid $[CH_3(CH_2)_9COOH]$ and undecylamine $[CH_3(CH_2)_{10}NH_2]$ are capable of forming, depending on the molar ratio and experimental conditions, a series of CA complexes, namely containing one, two, or three molecules of acid per amine molecule. Most of works on CTAB-containing CAS are devoted to their interaction with myristic acid (SA) $[CH_3(CH_2)_{12}COOH]$ having a rather lower length of alkyl chains as compared with CTAB [4–7]. It was found that lamellar phases, discs, or faceted vesicles [4] are formed depending on the composition. In those works, it was also found that the stable bilayers of CAS are formed at the molecular ratio of myristic acid to CTAB equal 2:1. The similar result was obtained for the pair of palmitic acid $[CH_3(CH_2)_{14}COOH]$ and CTAB [9]. These studies were conducted predominantly on water solutions of CAS, while the behavior of solid-state CAS has special interest for the development of fundamental science and its possible application. In our previous work [10], we addressed the molecular dynamics and the phase transitions in solid equimolar mixtures of a cationic surfactant

© J. BARAN, M. DROZD, T.A. GAVRILKO,
V.I. STYOPKIN, 2014

ISSN 2071-0194. Ukr. J. Phys. 2014. Vol. 59, No. 3

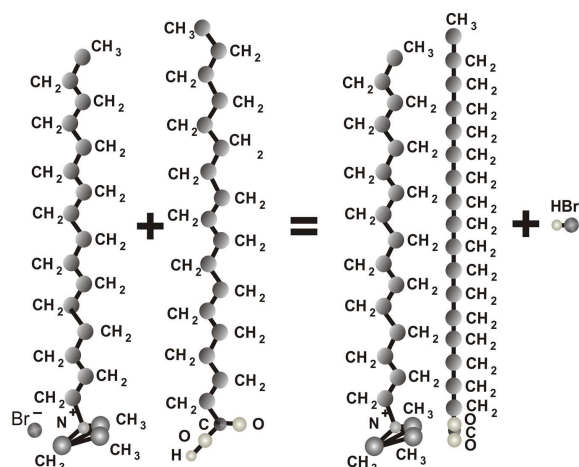


Fig. 1. Schematic representation of the formation of possible bitail CA supramolecular structure in a reaction between a cationic (CTAB) and anionic (SA) compounds

CTAB with stearic acid $\text{H}_3\text{C}-(\text{CH}_2)_{16}-\text{COOH}$, as an anionic surfactant. It was shown that the mixing of CTAB with SA results in the formation of a novel CA compound comprising both SA and CTAB remainders. The remarkable thermal stability of this compound was found with a melting point about 40 degrees higher as compared with original SA, which provides a molecular basis for promising applications of such class of supramolecular compounds in thermosensitive molecular devices. It was our interest to explore anionic and cationic surfactant mixtures with close alkyl chain lengths in order to study the effect of the molar ratio on the structure and properties of CA complexes. Since the properties of CAS depend on many factors, there is a need to investigate the solid state CAS structure, thermal properties, and phase behavior in more details. In the present work, we focus on the study of the SA:CTAB mixtures with different molar ratios. Several SA:CTAB molar ratios were employed ranging from 4:1 to 1:4. The prepared complexes were characterized, by using X-ray diffraction, FTIR spectroscopy, and DSC analysis. The structure, phase transitions, and molecular dynamics of the SA:CTAB solid complexes were studied.

2. Experimental

The initial compounds, CTAB (Fluka, 99%) and SA (Sigma-Aldrich), were used without any treatment. The SA:CTAB CA complexes were prepared from the ethanol solutions of the corresponding binary mixtures with different SA:CTAB molar ratios ranging

from 4:1 to 1:4. First, polycrystalline SA was dissolved in bidistilled ethanol heated up to 55–60 °C. The SA concentration in an ethanol solution was about 3 %wt. Then a required quantity of CTAB was added to the solution. The resulting mixture was kept at an elevated temperature for half an hour to ensure that the reaction between the components takes place. Then ethanol was left to fully evaporate, and the resulting CA complexes were obtained as a solid white precipitate.

The crystal structures of the obtained SA:CTAB complexes, as well their initial components CTAB and SA, were studied by X-ray powder diffraction. The XRD patterns were obtained at room temperature with a 139 DRON-3M X-ray diffractometer. $\text{Cu}_{K\alpha}$ radiation filtered with an Ni foil was used in these experiments.

The thermotropic properties of the prepared CA complexes were measured in the 20–130 °C temperature interval with a Perkin–Elmer DSC7 differential scanning calorimeter equipped with a CCA-7 low temperature accessory at a scanning rate of 8 °C/min. A small amount of the sample was enclosed in an aluminum pan hermetically sealed using a sample encapsulating press. Temperatures and enthalpies were calibrated using the standard indium sample. For comparison, the DSC curves for the initial compounds (CTAB and SA) were measured on heating and cooling cycles.

The temperature-variable FTIR transmission spectra of the investigated CA complexes, as well as pure CTAB and SA, were measured with a Bruker IFS-88 FTIR spectrometer in 400–4000 cm^{-1} spectral range and the temperature interval 20–150 °C. The spectral resolution was 1 cm^{-1} , and 128 scans were accumulated for each spectrum. The data processing was performed using the OPUS software. Samples for infrared spectroscopy were prepared as KBr-discpressed powders.

3. Results and Discussions

3.1. X-ray diffraction studies

The characteristic parts of diffraction patterns, taken at room temperature from the obtained CA compounds, are shown in Figs. 2 and 3. X-ray diffraction analysis shows that, for all SA:CTAB mixtures of different compositions (SA-CTAB molar ratio ranging from 4:1 to 1:4), the obtained CA compounds crys-

tallize in a lamellar structure similar to that of the initial components. In the low-angle region from 1.4 to 3.6 degrees, the lowest order diffraction peaks are observed at 1.87, 2.19, and 3.40 degrees. The peak positions at 2.19 and 3.40 degrees are close to those of the original compounds SA and CTAB, correspondingly, while the diffraction maxima at 1.87 degree, not observed either for pure SA or CTAB, gives evidence of a new structure formation. This structure was detected in our previous work [10] for equimolar SA:CTAB complexes with the same diffraction maxima at about 1.87 degrees.

Figure 2 shows that the lowest diffraction peak near 1.87 degree is observed for all obtained CAS, while the diffraction maximum at about 2.19 degree is detected only for pure SA and SA-rich CAS with SA:CTAB molar ratios of 4:1 and 2:1. This suggests that if the amount of SA is too large, the crystalline SA phase is observed, which may coexist with the lamellar phase of CA. The positions of the diffraction peaks near 1.87 and 2.19 degrees for different CAS are close to each other, the difference between them being less than 0.02 degree.

For CTAB-rich CAS with SA:CTAB molar ratios of 1:4 and 1:2, the XRD patterns are significantly different from those in the previous case (Fig. 3). First, the peak at 2.19 degree is absent, demonstrating that no crystalline SA phase is present anymore. Another characteristic feature of the pattern is the single peak observed at about 3.4 degrees, which is also present in pure CTAB, but not detected in SA-rich CAS. This peak is characteristic of the layered CTAB crystal structure. However, it should be noted that, in contrast to peaks shown in Fig. 2, the diffraction patterns in Fig. 3 show the evident difference in the peak widths and positions for CTAB and CAS. In Table, the widths and positions for the characteristic diffraction peaks of CAS under study are shown.

From the results of our X-ray study, we suggest that all studied SA:CTAB CA compositions do crystallize predominantly in a two-phase structure. The first of the coexisting CA phases is close to the bilayer structure of the equimolar 1:1 SA:CTAB complex [10], while the second one is similar to that of the excessive initial material. The relative amount of SA or CTAB phases in the CA structure is directly proportional to their molar fraction. This is demonstrated by the changes in the relative heights of the

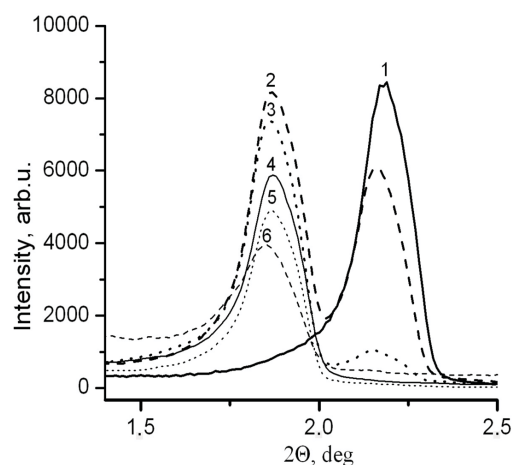


Fig. 2. X-ray diffraction patterns in the region near 2.0 degrees from SA (1) and the SA/CTAB CAS with different molar ratios: 4:1 (2), 2:1 (3), 1:1 (4), 1:2 (5), and 1:4 (6)

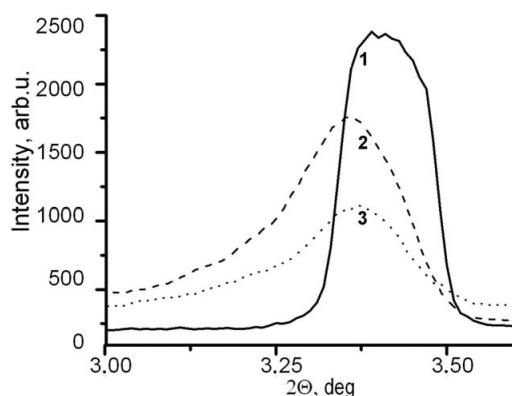


Fig. 3. X-ray diffraction patterns in the region near 3.4 degree for CTAB (solid) and the SA/CTAB CAS with molar ratios of 1:2 (dotted curve) and 1:4 (dashed curve)

diffraction peaks at 1.87 and 2.19 degrees, or near 3.4 degree, correspondingly. Interlayer distances, as determined from the position of peaks at 1.87 degree for the CA phase, are close for all obtained compounds and are about 4.64 nm. By contrast to [4–7, 9], our X-ray diffraction study did not reveal any phase with molar ratio SA:CTAB = 2:1. In this case, the excessive CTAB molecules will crystallize in a separate CTAB phase, and the corresponding reflection should be present in the diffraction patterns for SA:CTAB = 1:1 mixture. Note that no significant peak is observed at this angle for this mixture (see Table). X-ray diffraction results also show that the phase with molar ratio SA:CTAB = 3:1, similar

Characteristic lowest order peak positions (2θ), interlayer distances l , and full widths at half maximum FWHM of X-ray powder diffraction from SA, CTAB, and CAS with different SA:CTAB molar ratios

Sample	2θ , deg	l , nm	FWHM, deg	2θ , deg	l , nm	FWHM, deg	2θ , deg	l , nm	FWHM, deg
SA				2.18	3.98	0.17			
CTAB							3.41	2.54	0.14
4:1	1.87	4.64	0.17	2.16	4.02	0.16			
2:1	1.87	4.64	0.16	2.16	4.02	0.16			
1:1	1.86	4.66	0.17						
1:2	1.87	4.64	0.16				3.36	2.58	0.18
1:4	1.85	4.69	0.19				3.35	2.59	0.20

to that obtained in [8], is not formed in our study. The formation of such a phase would lead to the appearance of the diffraction peaks of the CTAB phase for the SA:CTAB mixture 2:1 too, that is not the case. Moreover, the absence of SA reflections for the mixtures of SA:CTAB = 1:1 and SA:CTAB = 1:2 also shows that the possible complexes with molar ratio SA:CTAB = 1:2 or 1:3 are not formed in all mixtures.

The formation of the 1:1 SA:CTAB phase in our experiment only presumably could be due to the closeness of the alkyl chain lengths of both components and is caused by a molecular packing factor. The observed small difference in the basic bilayer thicknesses (Table) can correspond to changes in the tilt angle of the chains in the crystal structure. The values of the tilt angles of the chains with respect to the layer plane were calculated from the basic bilayer thickness and the molecular length. These calculations were conducted, by assuming that alkyl chains in all CAS are in the all-*trans* form.

In the SA-rich CAS, the interlayer distance and the molecule tilt angles in the coexisting phase are close to those of the initial SA structure. By contrast to the CTAB-rich CAS, these characteristics of the second phase are slightly different from those of original CTAB. The tilt of the molecular long axis in CTAB makes up 65° , while, for CAS with SA:CTAB molar ratios of 1:2 and 1:4, it is about 67° . Moreover, the width of the diffraction peak observed near 3.4 degrees for these CAS indicates that a certain disorder of the layered structure takes place as compared with initial CTAB, which can be ascribed to a change in the state of alkyl chains within the surfactant bilayer.

3.2. DSC analysis

The DSC curves of SA:CTAB complexes measured in the heating scan are shown in Fig. 4. The transition temperatures of initial compounds – SA melting (71°C) and CTAB solid–solid phase transition (106°C) temperatures – are indicated by dotted lines. Our DSC results are similar to those reported in [11–13] for other long-chain CAS. As seen from Fig. 4, the obtained SA:CTAB compounds demonstrate a complicated thermal behavior with a number of successive phase transitions in the solid state. The observed phase behavior of the SA:CTAB complexes is quite different by depending on the molar ratio of their constituting components. The analysis of DSC data clearly indicates that the thermotropic behavior of the obtained SA:CTAB complexes is completely different from that of the initial components. Contrary to the original SA and CTAB with one sharp endothermic transition, the SA:CTAB complexes demonstrate a set of successive endothermic transitions seen in DSC curves at elevated temperatures under the heating run in the temperature interval $20\text{--}130^\circ\text{C}$. From the analysis of DSC scans, it follows directly that a two-phase separation occurs in solid SA:CTAB mixtures. The DSC curve in Fig. 4, *a* (4:1 SA:CTAB) shows the strong endothermic peak at 71°C superimposed with two peaks with small enthalpy at about 66 and 74°C . The broaden peak is also observed near 100°C , which corresponds to the full solid melting. The first peak could be assigned to the coexisting SA phase melting, while the other peaks nicely match the solid-solid transitions earlier observed for equimolar SA:CTAB complex [10]. This clearly confirms the two-phase nature of the solid

SA:CTAB complexes detected with X-ray diffraction. These observations were also confirmed by visual and polarized microscopic studies. The partial melting of this CA compound was detected at the temperature near 71 °C with its following full melting at 100 °C.

Figure 4, *e* presents similar DSC data for CAS with the 1:4 SA:CTAB molar ratio. This figure indicates the existence of the predominant single bulk phase of this CAS with the strong endothermic peak of a solid state phase transition at approximately 96 °C. According to [14], this is the temperature region of the CTAB solid–solid phase transition at 106 °C; however, the temperature of the observed transition is somewhat lower. Figure 4, *e* also indicates a weak shoulder centered at about 70 °C on the low temperature side of the main peak, suggesting that there may be another solid–solid phase transition in CAS. The optical microscopy study of this compound also revealed that the CTAB-rich CAS undergo a partial melting at an elevated temperature near 96 °C, while the remaining phase does not melt at this temperature. This observation is consistent with the thermotropic behavior of pure CTAB that does not melt at the temperature of the solid–solid phase transition at 106 °C, but decomposes at elevated temperatures near 260 °C [15]. Therefore, our DSC study confirms a two-phase segregation of the obtained CAS revealed by X-ray diffraction. Figure 4, *b–d* illustrates the DSC thermograms from the CA complexes with other SA:CTAB molar ratios. According to DSC, a number of phase transitions in CA complexes below the CTAB solid–solid phase transition is detected depending on the SA:CTAB molar ratio. The DSC peaks obtained for these CAS are usually broad and, in some cases, even bimodal. The structure of these peaks indicates that some other ordered structures may coexist with the lamellar 1:1 SA:CTAB phase. However, it is difficult to observe these other phases with DSC due to their small temperature stability. It should be noted that the corresponding heat flow peaks do not coincide with the transition points observed either for the initial SA or CTAB. Note that the X-ray diffraction patterns of these CAS also exhibit a phase separation behavior. This is a clear indication of the strong interaction between the anionic and cationic components in CAS and suggests that the obtained materials represent not simple binary mixtures of CTAB and SA, but a new supramolecular compound.

As is clear from the DSC, the thermotropic behavior of the studied solid CAS is rather complicated and includes several low temperature solid–solid phase transitions and a high-temperature melting. The melting point of the CAS with the molar ratio CTAB:SA \geq 1:1 is sufficiently higher than that of pure SA. For all studied SA:CTAB complexes, the two-phase segregation into the lamellar 1:1 SA:CTAB structure and the crystalline phase of excessive SA or CTAB is confirmed. To clarify the molecular structure of the SA:CTAB complexes and the nature of the observed successive thermotropic phase transitions, we have performed FTIR spectroscopy study. Temperature-induced changes in the molecular packing and the alkyl chain conformation in the solid phases of the CA complexes were defined after the detailed analysis of spectral parameters of the characteristic IR absorption bands.

3.3. FTIR spectroscopy

To characterize the head-group structure and the alkyl chain conformational order in the studied CA compounds with different SA:CTAB molar ratios, we measured FTIR absorption spectra of the obtained CAS and compared them with those of initial SA and CTAB. According to numerous FTIR spectroscopy studies on long-chain aliphatic compounds [16–20], the most informative IR absorption bands related to the head group structure of surfactant molecules are those originating from the carbon–oxygen vibrations that are observed in the 1500–1800 cm^{-1} region (Fig. 5, *a*). As follows from our FTIR study, the infrared spectra of SA:CTAB do not represent a simple superposition of the IR absorption spectra of the individual components, SA and CTAB. First, in FTIR spectra of pure SA, the C=O stretching band is observed at 1702 cm^{-1} with a smaller shoulder at 1687 cm^{-1} typical of H-bonded dimers [21–23]. The $\nu(\text{C}=\text{O})$ stretching vibration band is known to be highly characteristic of long-chain fatty acids, being usually observed in the 1690–1740 cm^{-1} interval. In the prepared CA compounds, one or several absorption bands are observed, in most cases, near the carbonyl stretching band of solid SA at about 1700 cm^{-1} . The new carbonyl band is considerably broader and shifted to higher wavenumbers. As is clearly seen from Fig. 5, *a*, the $\nu(\text{C}=\text{O})$ stretching bands of SA dimers in SA:CTAB mixtures gradu-

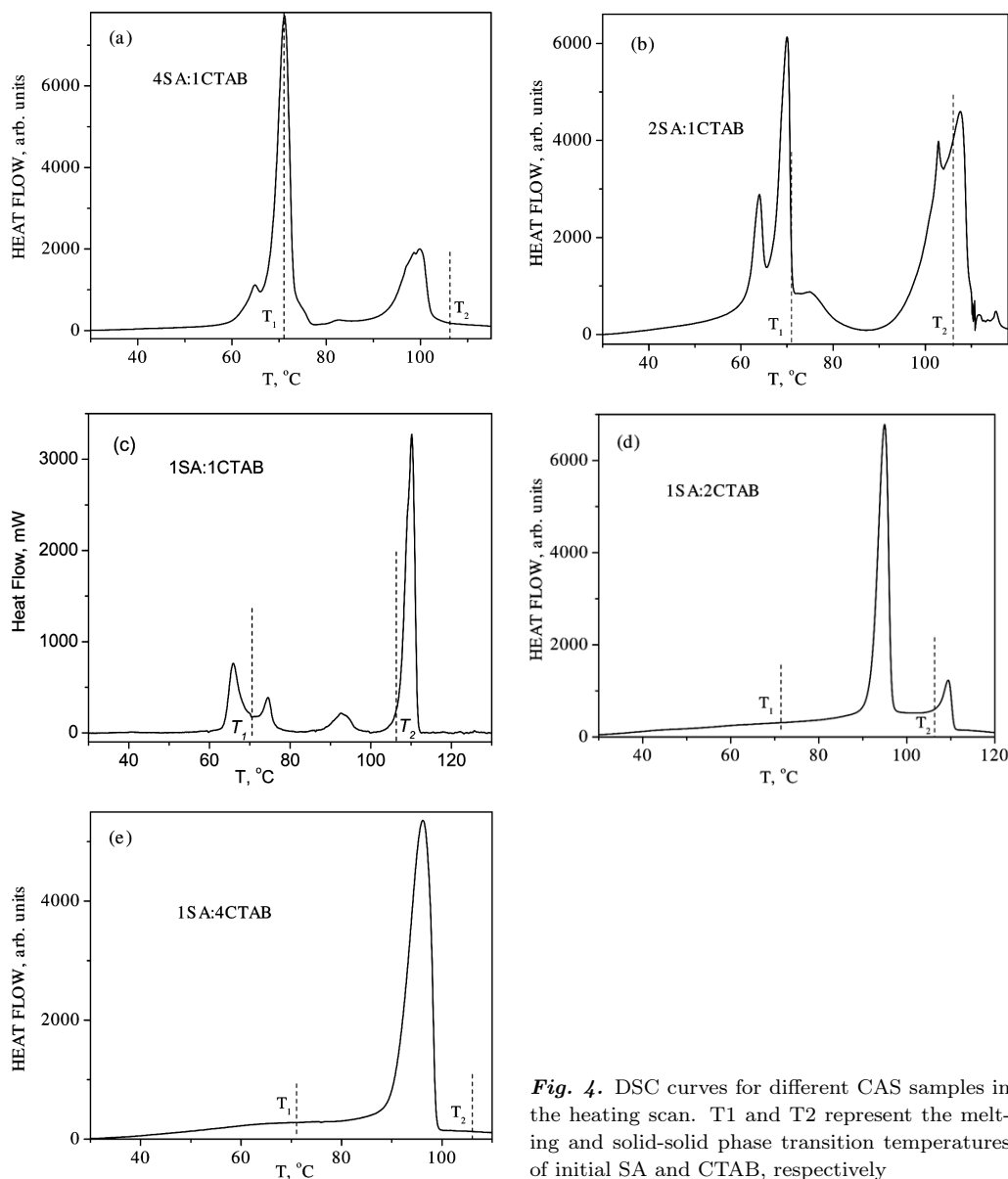


Fig. 4. DSC curves for different CAS samples in the heating scan. T₁ and T₂ represent the melting and solid-solid phase transition temperatures of initial SA and CTAB, respectively

ally disappear with a decrease in the SA molar ratio, and a new absorption band emerges at a higher frequency of 1714 cm^{-1} for CAS with 4:1 and 2:1 molar ratios. This observation, together with the disappearance of other absorption bands characteristic of dimer ring vibrations such as COO bending at 1300 cm^{-1} , suggests that SA molecules in the obtained CAS are in the monomeric form. The position of this band is similar to that observed earlier for the

1:1 SA:CTAB complex [10]. In the FTIR spectra of CTAB-rich CAS (Fig. 5, b), the carbonyl stretching band is shifted to even higher frequencies of 1724 , 1727 , and 1734 cm^{-1} for SA:CTAB molar ratios of 1:2 and 1:4 with higher CTAB content. The higher C=O frequency usually indicates weaker intermolecular interaction between the neighbor moieties [24] and suggests the increased separation between the adjacent acid fragments in the CA structure at lower SA

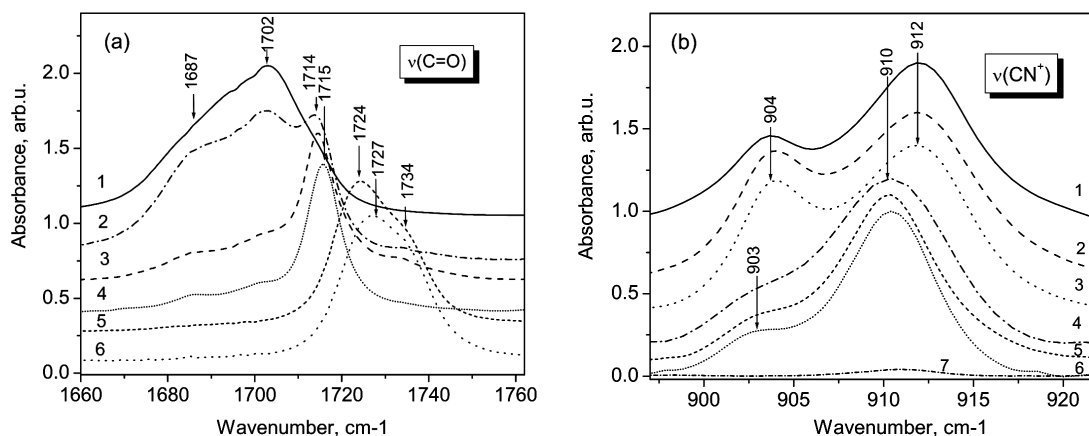


Fig. 5. Fragments of FTIR spectra in the region of $\nu(\text{C}=\text{O})$ (a) and $\nu(\text{CN}^+)$ (b) stretching vibrations for CA complexes with different SA:CTAB molar ratios as compared with initial SA and CTAB. (a): 1 – SA; 2 – 4:1; 3 – 2:1; 4 – 1:1; 5 – 1:2; 6 – 1:4; (b): 1 – CTAB; 2 – 1:4; 3 – 1:2; 4 – 1:1; 5 – 2:1; 6 – 4:1

molar fractions. The observed high-frequency shift of the $\nu(\text{C}=\text{O})$ stretching vibration band in the FTIR spectra of SA:CTAB complexes can be explained either by its strong coupling with $\delta(\text{CH}_3\text{-N}^+)$ bending vibrations of the CTAB moiety or by the influence of the electrostatic interaction with nearby CTAB head-groups $[\text{N}^+(\text{CH}_3)_3]$. Note that the bands characteristic of the CTAB-related $[\text{N}^+(\text{CH}_3)_3]$ head group, namely $\nu(\text{CN}^+)$ stretching vibrations at 912 and 904 cm^{-1} (Fig. 5, b), are all present in the spectra of CAS, being only slightly shifted, weakened, and broadened. This suggests that the head group of CTAB is slightly affected by the CAS formation. While it is difficult to arrive, from these data only, at a precise description of the rearrangement of the multiple carbon-oxygen bonds in the joined carboxylic acid $[\text{N}^+(\text{CH}_3)_3]$ head-group moiety, it is clear that the typical SA and CTAB bands have been affected by the complex formation. The position of the carbonyl band at a frequency higher than 1720 cm^{-1} indicates the presence of a carboxylic group that is much less hydrogen-bonded compared to that in fatty acid dimers.

Our FTIR results confirm the X-ray diffraction results showing the existence of well-ordered all-*trans* hydrocarbon chains in the solid phases of all studied CAS. This is proven by the existence of the methylene rocking and wagging propagation modes in the “fingerprint” spectral region (below 1700 cm^{-1}) of the FTIR spectra of all the studied CAS. In the 1180–1410 cm^{-1} spectral interval, the band progression of

methylene wagging vibrations is clearly seen (Fig. 6), which is characteristic of all-*trans* alkyl chain vibrations [24]. This confirms the perfect ordering of hydrocarbon chains in all studied solid SA:CTAB complexes at room temperature. It is clearly seen from Fig. 6 that, for the SA-rich CA aggregates, the observed band progression represents a superposition of the corresponding progressions of initial SA and the equimolar SA:CTAB complex (Fig. 6, b). For CTAB-rich CAS, the band progression is similar to that of the equimolar complex (with no signs of SA due to its low concentration). However, the bands positions and their intensities in the progression are quite different. Since the intensity of the bands in the progression of methylene wagging vibrations is known to be sensitive to the head group polarity [25], this suggests that the head group structures in CA complexes with different molar ratios are fairly different. In addition, in the FTIR spectra of all CAS, a splitting is observed for the methylene scissoring mode (with two components centered at 1472 cm^{-1} and 1463 cm^{-1}) and the methylene rocking mode (with two components at 720 cm^{-1} and 730 cm^{-1}). It is known that the splitting of molecular absorption bands into several components with different polarizations (known as a factor-group or Davydov splitting of vibrational excitons) appears due to the ordered crystalline environment and is generally observed for crystals with several molecules per unit cell.

As was shown in our previous papers [23, 25–26], the appearance of the Davydov splitting in the IR

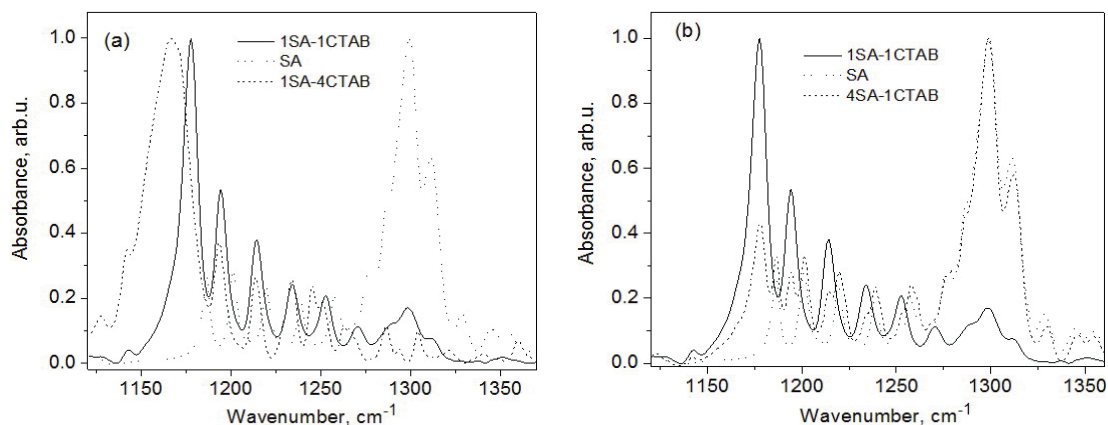


Fig. 6. Fragments of FTIR spectra in the region of CH₂ wagging propagation modes for CA complexes with 1:4 (a) and 4:1 (b) SA:CTAB molar ratios as compared with initial SA and 1:1 SA:CTAB complex

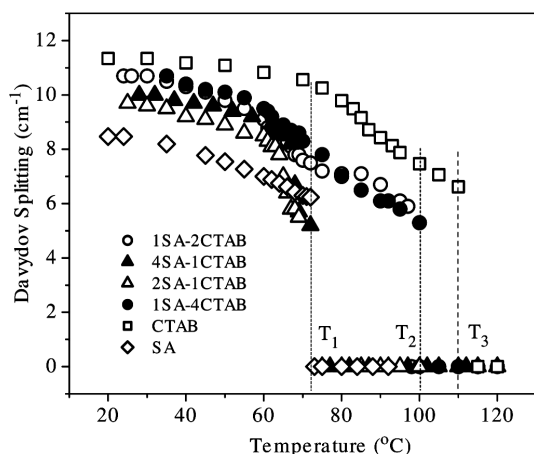


Fig. 7. Temperature dependence of the Davydov splitting of the CH₂ rocking mode (720 cm⁻¹) in FTIR spectra of different CAS and original SA and CTAB

spectra of some solid-phase long-chain aliphatic compounds is related to the fact that the packing of their methylene chains can be described by an orthorhombic crystal sub-cell. This unit cell contains two translationally non-equivalent chain fragments, each containing two methylene groups (-CH₂-). The dipole moments corresponding to their vibrations are mutually perpendicular, being parallel to the crystal cell axes, a_s and b_s . In our study, the above-mentioned observation of the Davydov splitting suggests the orthorhombic packing of methylene chains in the solid phase of all SA:CTAB complexes. The temperature dependence of the Davydov splitting value was proven to be a powerful tool for studies of the lattice dynamics and phase transitions

in molecular crystals. Changes in the resonance dynamic intermolecular interaction in the temperature-induced orientationally disordered phases are expected. In particular, it was shown that the Davydov splitting of the CH₂ rocking mode of alkyl chains drops to zero at the orthorhombic-to-hexagonal phase transition.

To clarify the physical nature of the observed phase transitions, we focused on the analysis of the temperature-variable FTIR spectra of CA complexes. Figure 7 shows the temperature dependence of the Davydov splitting (DS) value for the CH₂ rocking vibrations band in the FTIR spectra of SA:CTAB complexes as a function of the temperature. One can see that the DS value gradually decreases with the temperature for all studied complexes, the decrease being more rapid for SA-rich CAS than for CTAB-rich ones. Since the DS value is inversely proportional to r^3 , this observation suggests that a significant change in the packing of alkyl chains in CA complexes is developed at elevated temperatures. The DS value drops to zero at $T_1 = 72$ and $T_2 = 100$ °C for SA-rich and CTAB-rich CA compositions, respectively, while the corresponding transition in original CTAB occurs at $T_3 = 110$ °C. This observation suggests a change in the packing of methylene chains from the orthorhombic into another crystalline phase at elevated temperatures. Note that the SA:CTAB solid-solid phase transition points defined from the FTIR spectroscopy are close to the first low-enthalpy transition temperature for the corresponding complexes defined from DSC measurements (Fig. 4). Considering that, at these transition temperatures, a conforma-

tional disorder of alkyl chains is developed, all these changes indicate the solid-solid nature of the corresponding phase transitions. It is worth to mention a drastic broadening of the corresponding Davydov splitting components (by about 40%) under the solid-solid phase transition. This suggests that, in the newly formed phase, the methylene chains are in a dynamically disordered state or hindered rotation and are packed in the so-called hexagonal or rotary phase [25]. It is of importance that the transition point to the rotary phase is higher for the CTAB-rich CAS as compared with SA-rich ones, which suggests a higher stability of their structures. This may be due to a complicated interplay between steric factors and electrostatic effects in crystalline CA aggregates. In the CTAB-rich CAS, the alkyl chains are more tightly packed, so the increase in the conformational disorder must be somewhat restricted. Thus, the successive low-enthalpy endothermic phase transitions occurring in SA:CTAB complexes are connected with a cooperative dynamical disorder in their structures due to conformational changes and hindered molecular rotations of alkyl chains. As we have already mentioned, the melting temperatures of the SA:CTAB complexes are much higher (up to 40 °C in the 1:1 SA:CTAB complex) as compared with that of initial SA. This suggests that the incorporation of CTAB molecules with a positively charged bulky head group into the SA structure contributes to electrostatic interactions in the ionic layer, by significantly improving the thermal stability of the SA crystal lattice.

4. Conclusions

The solid phase complexes of a cationic surfactant cetyltrimethylammonium bromide with stearic acid as an anionic surfactant have been prepared with different SA:CTAB molar ratios ranging from 4:1 to 1:4. The prepared catanionic surfactants were characterized with the use of X-ray powder diffraction, DSC analysis, and temperature-variable FTIR spectroscopy. It is shown that the obtained CA complexes in the solid state are assembled into a phase-segregated layered structure. The obtained results suggest that the aggregate composition is close to equimolar both at the acid-rich and CTAB-rich sides of the phase diagram with the coexisting excessive SA or CTAB phase, which is confirmed by

FTIR spectroscopy. According to DSC, a number of phase transitions in CA complexes below the CTAB solid-solid phase transition temperature are detected. Characteristics of these transitions depend on the SA:CTAB molar ratio. With the use of FTIR spectroscopy, the physical nature of the observed phase transitions is clarified. It is shown that, below the solid-solid phase transition temperature, a change in the packing of methylene chains from the orthorhombic to dynamically disordered state (the so-called hexagonal or rotary phase) takes place. The obtained SA:CTAB complexes with molecular ratios $\text{CTAB:SA} \geq 1$ are significantly much more stable in the solid state than the pure SA, which results, in particular, in the higher melting point of these complexes.

The authors are deeply thankful to Prof. V.G. Il'in for support in providing the X-ray measurements. The financial support from the National Academy of Science of Ukraine under the program "Nanophysics and Nanoelectronics" (project No. VC-157) is gratefully acknowledged.

1. R.M.F. Fernandes, E.F. Marques, B.F.B. Silva, and Y. Wang, *J. Mol. Liq.* **157**, 113 (2010).
2. T. Bramer, N. Dew, and K. Edsman, *J. Pharm. Pharmacol.* **59**, 1319 (2007).
3. S.M. Moghimi, A.C. Hunter, and J.C. Murray, *FASEB J.* **19**, 311 (2005).
4. T. Zemb, D. Carriere, K. Glinel, M. Hartman, A. Meister, C. Vautrin, N. Delrome, A. Fery, and M. Dubois, *Colloids and Surf. A* **303**, 37 (2007).
5. A. Stocco, D. Carriere, M. Cottat, and D. Langevin, *Langmuir* **26**, (13), 10663 (2010).
6. Y. Michina, D. Carriere, T. Charpentier, R. Brito, E.F. Marques, J.-P. Douliez, and T. Zemb, *J. Phys. Chem. B* **114**, 1932 (2010).
7. E. Maurer, L. Belloni, T. Zemb, and D. Carrière, *Langmuir* **23**, 6554 (2007).
8. C. Sun, M.J. Bojdys, S.M. Clarke, L.D. Harper, A. Jefferson, M.A. Castro, and S. Medina, *Langmuir* **27**, 3626 (2011).
9. Y. Michina, D. Carrière, C. Mariet, M. Moskura, P. Berthault, L. Belloni, and T. Zemb, *Langmuir* **25**, 698 (2009).
10. T.A. Gavrilko, G.O. Puchkovska, V.I. Styopkin, T.V. Bezrodna, V.G. Il'in, J. Baran, and M. Drozd, *Ukr. J. Phys.* **58**, 636 (2013).
11. V. Tomašić, S. Popović, and N. Filipovic-Vinceković, *J. of Colloid and Interf. Sci.* **215**, 280 (1999).

12. M.L. Lynch, F. Wireko, M. Tarek, and M. Klein, *J. Phys. Chem. B* **105**, 552 (2001).
13. N. Filipovic-Vinceković, I. Pucić, S. Popović, V. Tomašić, and D. Težak, *J. of Colloid and Interf. Sci.* **188**, 396 (1997).
14. T. Bezrodna, G. Puchkovska, V. Styopkin, J. Baran, M. Drozd, V. Danchuk, and A. Kravchuk, *J. of Mol. Struct.* **973**, 47 (2010).
15. K. Iwamoto, Y. Ohnuki, K. Sawada, and M. Seno, *Mol. Cryst. Liq. Cryst.* **73**, 95 (1981).
16. W. Wu, Y. Wang, and H.-S. Wang, *Vibr. Spectr.* **46**, 158 (2008).
17. Q. Wang Q, W. Xu, and B. Zhao, *Spectroch. Acta Part A* **59**, 793 (2003).
18. A. Imanishi, R. Omoda, and Y. Nakato, *Langmuir* **22**, 1706 (2006).
19. D. Hadži, J. Grdadolnik, and A. Meden, *J. of Mol. Struct.* **381**, 9 (1996).
20. D.C. Lee and D. Chapman, *Biosci. Reports* 6(3), 235 (1986).
21. J.B. Peng, G.T. Barnes, and I.R. Gentle, *Adv. in Colloid and Interf. Sci.* **91**, 163 (2001).
22. B.F.B. Silva, E.F. Marques, U. Olsson, and R. Pons, *Langmuir* **26**(5), 3058 (2010).
23. G.O. Puchkovska, S.P. Makarenko, V.D. Danchuk, and A.P. Kravchuk, *J. of Mol. Struct.* **744-747**, 53 (2005).
24. L.J. Bellami, *The Infra-Red Spectra of Complex Molecules* (Wiley, New York, 1958).
25. G.O. Puchkovska, *Manifestation of Structure, Dynamics, and Polymorphism in Vibrational Spectra of Molecular crystals*, Thesis of the Doctor Dissertation in Phys. and Math. (Kyiv, 1988).
26. S.P. Makarenko, G.O. Puchkovska, E.N. Kotelnikova, and S.K. Filatov, *J. of Mol. Struct.* **704**, (1-3), 25 (2004).

Received 25.09.13

Я. Баран, М. Дрозд, Т.А. Гаврилко, В.І. Стъопкін

СТРУКТУРА, МОЛЕКУЛЯРНА ДИНАМІКА
ТА ТЕРМОТРОПНІ ВЛАСТИВОСТІ КАТАНІОННИХ
З'ЄДНАНЬ НА ОСНОВІ СТЕАРИНОВОЇ
КИСЛОТИ ТА ЦЕТИЛТРИМЕТІЛАММОНІУМ
БРОМІДУ ПРИ РІЗНИХ МОЛЯРНИХ
СПІВВІДНОШЕННЯХ

Резюме

З метою отримання нових перспективних молекулярних матеріалів синтезовано та досліджено катаніонні речовини на основі комплексних з'єднань цетилтриметіламмоніум броміду (СТАВ) $[\text{H}_3\text{C}-(\text{CH}_2)_{15}-\text{N}^+(\text{CH}_3)_3]\text{Br}^-$ та стеаринової кислоти (СА) $(\text{H}_3\text{C}-(\text{CH}_2)_{16}-\text{COOH})$ при молярних співвідношеннях компонент від 4:1 до 1:4. Дослідження рентгенівської дифракції показали, що у всіх випадках утворюється двофазна система, причому обидві фази мають ламелярну структуру. Сформовані комплекси складаються із катаніонної еквімолярної складової (СТАВ:СА = 1:1) та надлишкової фази (СТАВ або СА), що підтверджується даними FTIR. На відміну від вихідних речовин в отриманих комплексах з ростом температури відбувається декілька фазових переходів в твердому стані, параметри яких залежать від співвідношення компонент. Сформовані комплекси (зокрема, еквімолярна фаза) характеризуються підвищеною стабільністю в порівнянні із чистою стеариновою кислотою. Обговорюється вплив структури та складу комплексів на фазову діаграму та молекулярну динаміку комплексів СТАВ + СА.